

## LARGE EDDY SIMULATION OF TURBULENT FLOWS IN COMPOUND CHANNELS

C. M. Xavier, carla.xavier@ufrgs.br  
A. P. Petry, adrianep@mecanica.ufrgs.br  
S. V. Möller, svmoller@ufrgs.br

PROMEC – Programa de Pós Graduação em Engenharia Mecânica  
UFRGS – Universidade Federal do Rio Grande do Sul  
Porto Alegre, RS, Brazil

**Abstract.** *Compound channels are found in several branches of the engineering, from rod bundles of nuclear reactors and heat exchangers to irrigation channels with flood plains in hydraulic engineering, or finned channels for cooling of electronic devices. This paper presents a numerical investigation of the developing flow in a compound channel formed by a rectangular main channel and a slot in one of the sidewalls. A three-dimensional Large Eddy Simulation computational code with the classic model of Smagorinsky is introduced, where the transient flow is modeled through the conservation equations of mass and momentum of a quasi-incompressible, isothermal continuous medium. Finite Element Method is used and Taylor-Galerkin scheme is applied for time and space discretization and to link governing equations. The discretization of the computing domain is made by means of linear hexahedral elements. Numerical results of velocity profile show the development of a shear layer in good agreement with experimental results obtained with Pitot tube and hot wires.*

**Keywords:** *Turbulent Flow, Compound Channels, Finite Elements, Subgrid Scale Models, Hot wires.*

### 1. INTRODUCTION

The cross section of a compound channel is formed by a narrow region (gap) connected to a wider one, or, conversely, a narrow region connecting two wider regions. In nuclear reactors, the narrow gap between the rods connects parallel sub-channels. The investigation of the turbulent flow in this channel type show peculiar characteristics in relation to stress distribution and the coefficient of turbulent heat transfer on the region between two channels.

“Experimental measurements in a single line rod bundle, showed high values of turbulence intensity for the axial and azimuthal components of velocity in the region of the gap and a strong relationship between the increase in these quantities and decreasing of the distance between the tubes” (Möller, 1991). Fluctuations of the different velocity components showed a quasi-periodic behavior close to gap, exactly as identified previously in Rowe et al. (1974), which suggested that these pulsations of the flow were responsible for the increase in turbulent intensities along the gap.

The velocity distribution and characteristics of the turbulent flow in channels with rectangular gap in the sidewall at a range of Reynolds numbers from 2300 to 100000 was investigated experimentally by Meyer and Rehme (1995). Flow visualizations showed consistent, stable and equally spaced structures transported by the mean flow inside the gap.

The characteristics of the turbulent flow in two channels connected by a rectangular gap, near the upper wall, using large eddy simulation with periodic boundary conditions in the main flow direction was presented in Biemüller et al. (1996). The height and width of the channel were respectively 180 mm and 331.6 mm with a length of 504 mm. The gap that connects the two main channels has height  $d$  and width  $g$  of 10.20 mm and 40.6 mm respectively, being the ratio  $g/d = 4$ . The Reynolds number of the simulation ranged from 3300 to 580000. The results showed peak Reynolds stresses along the gap and large vortices carried by the mean flow rotating in opposite directions, as modeled by Möller (1991).

Merzari et al. (2008), report a detailed LES study to capture the pulsating flow in compound channels in a rectangular duct forming two wide regions connected by a gap is presented.

In his Thesis, Goulart (2009), established the relation between the distribution of velocity and velocity fluctuations and the mixing layer theory and proposed a Strouhal number definition to describe the dimensionless frequency of the pulsations

Recently, Meyer (2010), made a comprehensive review of the flow pulsations in rod bundles, including the knowledge obtained in several types of compound channels. He concludes that the origin of this phenomenon is still disputed and that there is an analogy between flow pulsations and the mixing layer formed by two flows with different velocities merging from a split plate.

The purpose of this paper is to present a numerical investigation for the study of the developing turbulent flow in compound channels. The numerical code employs the finite element method to perform large eddy simulation of the

transient, quasi-incompressible, three-dimensional channel flow (Petry and Awruch, 2006), using the Smagorinsky model, with eight node hexahedral elements solved by an explicit Taylor-Galerkin scheme. The geometry of the channel consists on a main channel connected to a gap on a side wall. Results are compared with experimental results obtained with Pitot tube and hot wires in an aerodynamic channel.

## 2. TEST SECTION AND COMPUTATIONAL DOMAIN

The investigations were made in a rectangular channel with 146 mm height and 193 mm in width, with a gap in the side wall in which the flow develops. The gap was 2000 mm long with a depth  $d = 80$  mm and width  $g = 20$  mm, thus having a  $d/g$ -ratio equal to 4. The working fluid used is air at room temperature, driven by a centrifugal blower passing through a diffuser, a homogenizer and two screens, reaching the test section with turbulence intensity less than 1%. At 150 mm downstream of the screens a Pitot tube is located, to measure the reference velocity  $U_{REF}$ , which is approximately equal to the mean velocity in the channel.

The Reynolds numbers of experiment and simulation were calculated using the mean velocity of the flow in the test section and its hydraulic-diameter,  $D_h = 131.08$  mm, ranging from  $Re = 100$  to  $Re = 85,000$ .

Figure 1 (a) shows a schematic view of the test section studied, where the red line shows the location of the gap while Fig. 1 (b) and (c) shows schemes of the cross section with location of hot wire measurements.

The average values of axial component of velocity were measured using a Pitot tube with outside diameter of 1.25 mm. The velocity fluctuations of the axial components  $u$ , cross  $w$ , were evaluated via hot wire anemometry, using a constant temperature probe DANTEC StreamLine. In the simultaneous measurement of two velocity components a double wire probe was used, which has a wire perpendicular to the main flow and a slant ( $45^\circ$ ) wire. In the calibration of this probe, the method proposed by Collins and Williams (1959), was used, with modifications reported by Olinto and Möller (2004).

The Pitot tube and hot wire probe were moved along the symmetry line of the channel by means of a tri-axial positioner. In this work, the axial velocity component,  $u$ , is parallel to main flow direction and the transverse component,  $w$ , is parallel to the symmetry line. Data acquisition of hot wire signals was done using a 16 bit analog digital converter board (National Instruments 9215-A), and a sampling frequency of 3 KHz. The length of the records was 21.84 s. The average error in determining the velocity with the hot wire anemometer was approximately 3%.

In the computational domain, the channel is represented by a uniform mesh composed by 85,644 nodes. The channel geometry and the mesh are shown respectively in Figure 2 and represent accurately the test section.

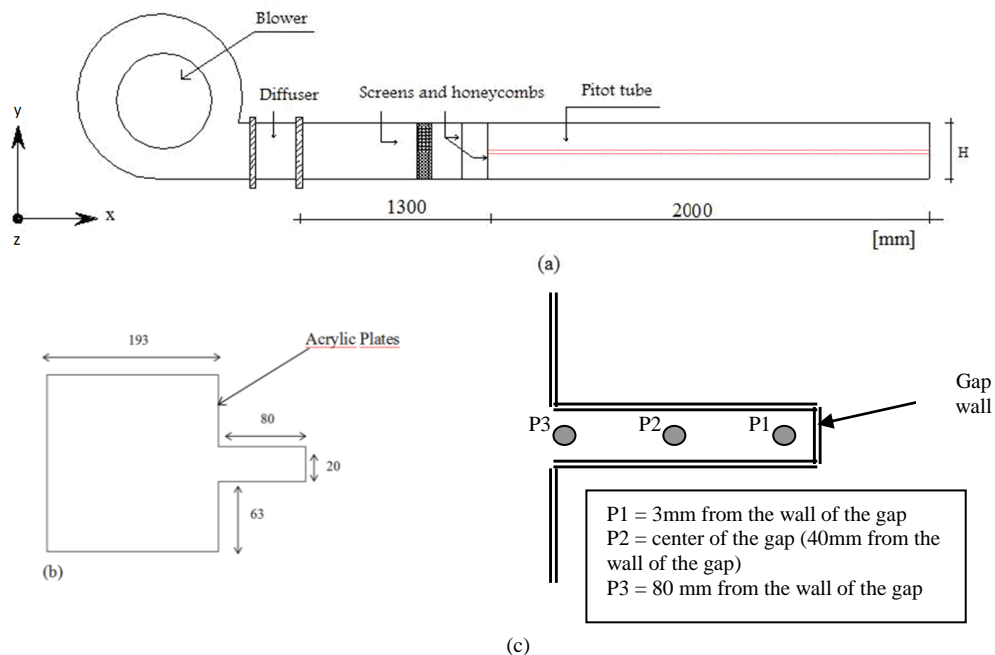


Figure 1. Schematic view of the test section:

a) side view of the channel, b) cross section of the channel, c) location of hot wire measurements.

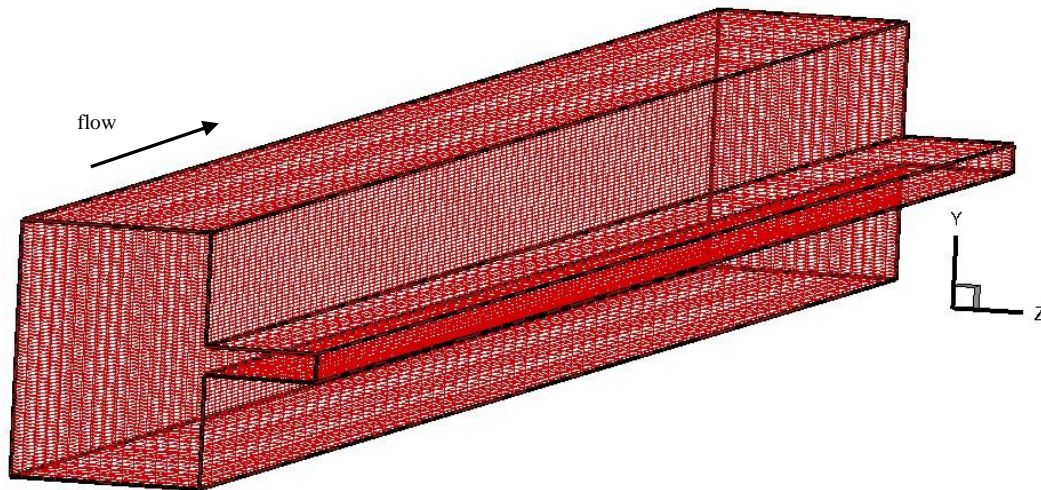


Figure 2. Computational grid

### 3. MATHEMATICAL AND NUMERICAL ASPECTS

#### 3.1. Governing equations

In large eddy simulations, balance equations for mass, energy and momentum of a viscous, quasi-incompressible, three-dimensional, transient and isothermal flow of a Newtonian fluid (Kawahara and Hirano, 1983; Findikakis and Street, 1982 and Petry and Awruch, 2006) are decomposed into large-scale field (identified by the bar over the variable) and subgrid scale field (identified by the apostrophe). Filtered velocity and pressure are

$$v_i = \bar{v}_i + v'_i \quad p = \bar{p} + p' \quad (1)$$

Filtered equations of mass and momentum are given by:

$$\frac{\partial \bar{p}}{\partial t} + C^2 \frac{\partial}{\partial x_j} (\rho \bar{v}_j) = 0 \quad (2)$$

$$\begin{aligned} \frac{\partial}{\partial t} (\rho \bar{v}_i) + \frac{\partial}{\partial x_j} (\rho \bar{v}_i \bar{v}_j) + \frac{\partial \bar{p}}{\partial x_j} \delta_{ij} - \frac{\partial}{\partial x_j} \left\{ \nu \left( \frac{\partial}{\partial x_j} (\rho \bar{v}_i) + \frac{\partial}{\partial x_i} (\rho \bar{v}_j) \right) + \frac{\lambda}{\rho} \left( \frac{\partial}{\partial x_k} (\rho \bar{v}_k) \right) \delta_{ij} \right\} \\ + \frac{\partial}{\partial x_j} \left\{ \rho (L_{ij} + C_{ij} + \overline{v'_i v'_j}) \right\} - f_i = 0 \end{aligned} \quad (j = 1, 2, 3) \text{ in } \Omega \quad (3)$$

With boundary conditions:

$$v_i = \hat{v}_i \quad \text{in } \Gamma_v \quad (4)$$

$$\left\{ \left[ -\bar{p} + \frac{\lambda}{\rho} \frac{\partial}{\partial x_k} (\rho \bar{v}_k) \right] \delta_{ij} + \nu \left[ \frac{\partial}{\partial x_j} (\rho \bar{v}_i) + \frac{\partial}{\partial x_i} (\rho \bar{v}_j) \right] \right\} n_j = t_i \quad \text{in } \Gamma_t \quad (5)$$

and the corresponding initial conditions:

$$v_i = \hat{v}_{i0} \quad \text{in } t = 0, \Omega \quad (6)$$

$$p = \hat{p}_0 \quad \text{in } t = 0, \Omega \quad (7)$$

Where:

$\rho \rightarrow$  fluid density (kg/m<sup>3</sup>)

$v_i \rightarrow$  velocity component in direction i (m/s)

$x_i \rightarrow$  coordinate in i direction (m)

$\delta_{ij} \rightarrow$  Kronecker delta

$\hat{v}_i \rightarrow$  velocity i values prescribed on the boundary indicated (m/s)

$n_j \rightarrow$  director cosine of the vector normal to the boundary

$t_i \rightarrow$  prescribed values of surface forces on the boundary (N)

$\mu \rightarrow$  Coefficient of dynamic viscosity of the fluid (Pa.s)

$\lambda \rightarrow$  Coefficient of viscosity of the fluid volume (Pa.s)

$C \rightarrow$  velocity of sound propagation (m/s)

$\nu \rightarrow$  kinematic viscosity (m<sup>2</sup>/s)

$\bar{v}_i \rightarrow$  component, corresponding to large scales, the velocity vector in the direction xi (m/s).

$\bar{p} \rightarrow$  Pressure component corresponding to large scales (Pa).

$v'_i \rightarrow$  velocity component in the direction  $x_i$ , corresponding to the subgrid scales (m/s)

$L_{ij} = \overline{\bar{v}_i \bar{v}_j} - \bar{v}_i \bar{v}_j \rightarrow$  terms of Leonard.

$C_{ij} = \overline{v_i v_j'} + \overline{v_i' v_j} \rightarrow$  cross terms.

$\overline{v_i' v_j'} \rightarrow$  Reynolds tensor subgrid scale (m<sup>2</sup>/s<sup>2</sup>).

$\Omega \rightarrow$  problem domain

$\Gamma_v \rightarrow$  face boundary with prescribed velocity

$\Gamma_t \rightarrow$  face with natural boundary condition

Leonard and cross terms  $L_{ij}$  and  $C_{ij}$  has been neglected in Findikakis and Street (1983). Petry and Awruch (2006) confirm that the inclusion of these terms do not significantly affect the results and increase around 20% processing time. Therefore, neglecting Leonard's and cross terms, Eqs. (2) and (3), with the initial and boundary conditions given by Eq. (4), (5), (6) and (7) are the governing equations. For the solution of the system a subgrid scale model must be used.

The quasi incompressible analysis assumes a constant density throughout the flow domain, but the sound velocity is not considered infinite. As a result of this consideration, time derivative of the pressure appears in mass conservation equation (Eq. 2), simplifying the handling of the equation system (Petry and Awruch, 2006).

### 3.2. Subgrid Scale Models

Both models are implemented based on the concept of turbulent viscosity and using the Boussinesq hypothesis, the Reynolds stress subgrid scales are given by:

$$\overline{-v_i'v_j'} = \nu_t \left( \frac{\partial \overline{v_i}}{\partial x_j} + \frac{\partial \overline{v_j}}{\partial x_i} \right) \quad (8)$$

where  $\nu_t$  is the turbulent viscosity.

For incompressible flows, this equation is usually modified by introducing a subgrid scale kinetic energy term to make the model compatible with the mass conservation equation for incompressible flows (Hinze, 1975). But in this work, the equation of continuity is modified for quasi-incompressible flows, maintaining, therefore, Eq. (8) in its original form.

The Smagorinsky model has been traditionally used to represent the effect of the subgrid scales in large eddy simulation (Findikakis and Street, 1983; Petry and Awruch, 2006), being a turbulent viscosity model in which the Reynolds stresses are given by a subgrid scale, Eq. (8), and the turbulent viscosity is defined as:

$$\nu_t = C_s^2 \overline{\Delta}^2 |\overline{\mathbf{S}}| \quad (9)$$

Where  $C_s$  is the Smagorinsky constant and other terms are given by:

$$|\overline{\mathbf{S}}| = \sqrt{2\overline{S_{ij}S_{ij}}} \quad (10)$$

$$\overline{S_{ij}} = \frac{1}{2} \left( \frac{\partial \overline{v_i}}{\partial x_j} + \frac{\partial \overline{v_j}}{\partial x_i} \right) \quad (11)$$

$$\overline{\Delta} = \sqrt[3]{\prod_{i=1}^3 \Delta x_i} \quad (12)$$

As boundary conditions at the entrance, a uniform velocity profile was adopted ( $v_1 = V(y)$ ,  $v_2 = 0$ ,  $v_3 = 0$ ) and non-slip condition ( $v_1 = v_2 = v_3 = 0$ ) for all walls. For the outlet, natural boundary conditions ( $t_1 = t_2 = t_3 = 0$ ) were prescribed (see Eq. (5)). The initial conditions used are  $v_1 = U_{ref}$  (steady value),  $v_2 = v_3 = p = 0$ .

### 3.3 Numerical Simulation

Large eddy simulations of the three-dimensional flow in the compound channel investigated were performed with Reynolds number  $Re=100$ ,  $3300$  and  $10000$ . When a simulation is completed, the resulting velocity field is used as initial condition for the next simulation with a higher Reynolds number.

The code uses a parallel processing OpenMP technique, which allows the solution of large and complex problems and has the advantage of automatically initiate a scan of available processors, distributes tasks and dynamically adjusts the partitions for the number of processors and each processor load. The language of the code is FORTRAN 95, using high performance techniques. To ensure its portability and facilitate changes the code has a modular structure (each module is a set of subroutines stored in a different file), allowing a selective compilation by adding or deleting routines.

The time step used for  $Re = 100$  was  $5 \times 10^{-4}$  s,  $Re = 3300$  and  $Re = 10000$  it was  $1 \times 10^{-5}$  s, the Smagorinsky constant,  $C_s$ , was 0.23.

## 4. RESULTS

Figure 3 shows the axial velocity contours obtained in channel, 50mm before outlet for  $Re = 3300$ . It is observed a region of maximum velocity occurring in the main channel and a level of nearly constant velocity in the gap region. The excessive deflection of isovelocity lines suggests that the simulation exaggerates the secondary flows; however, these results are in accordance with experimental results in Meyer and Rehme (1995) and recent simulations in Home (2009). The presence of coherent structures is firstly observed by the presence of peaks in spectra of axial and transversal velocity fluctuations (toward the gap). By using the Strouhal number definition proposed in Meyer and Rehme (1995), given by

$$\text{Str} = \frac{f}{U_c} \sqrt{g \cdot d} \tag{13}$$

the frequency obtained, with  $\text{Str}=0.066$ , for the Reynolds number investigated is  $f=16.5$  Hz. Figure 4 shows maximal values of the spectra at 25Hz, higher than the calculated value, but still in the same order of magnitude.

Figure 5 shows the axial mean velocity profiles along the symmetry line of the channel are shown as a function of the position  $z/d = 1$ , corresponds to the edge of the gap. In spite of the difference in the Reynolds number, the code underestimates the flow velocity in the gap region. This is attributed to the coarse grid and due to the Smagorinsky model employed. The results in this graph were not compared to  $\text{Re} = 85000$  because of the time step of integration is very small, which results in long processing time in such high Reynolds numbers.

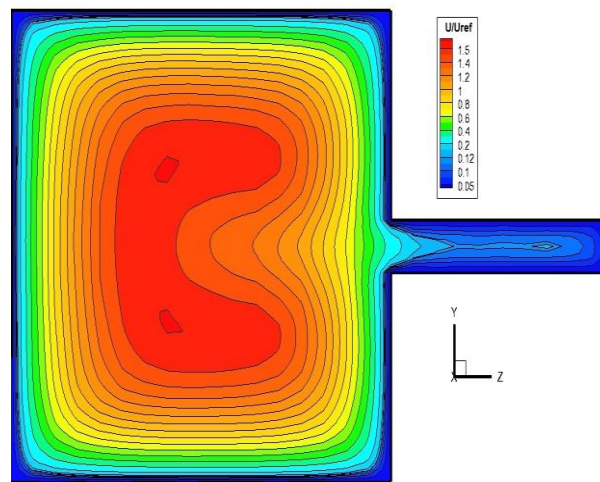


Figure 3. Contours of axial mean velocity, 50 mm upstream of the channel outlet, ( $X/L = 0.98$ ) -  $\text{Re} = 3300$  - numerical.

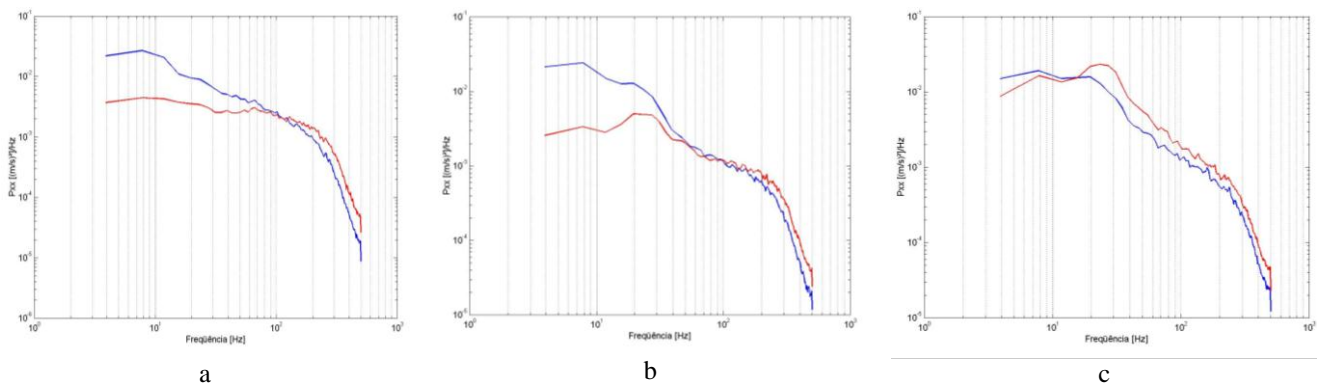


Figure 4. Autospectral density of axial (blue) and transversal (red) velocity fluctuation: a) P1; b) P2; c) P3. Location in Fig. 1-c.

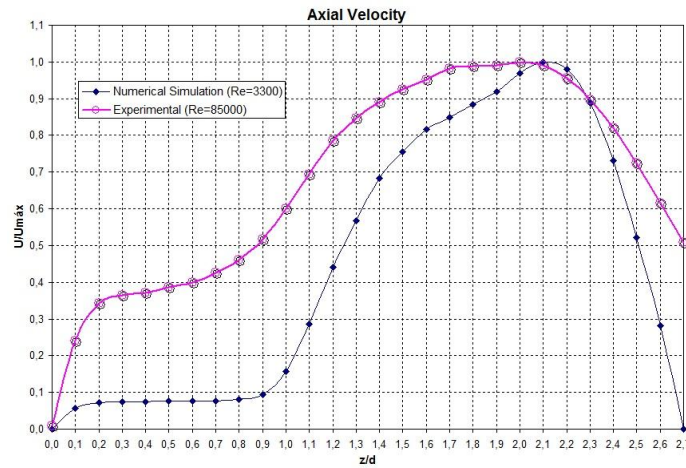


Figure 5. Axial velocity profiles as function of the dimensionless parameter  $z/d$ .

Figure 6 shows the normalized by the average friction velocity  $U\tau$ , turbulent shear stress  $U'W'$  along the symmetry line. The shear stress  $U'W'$  parallel to the gap is zero at the symmetry line between the two channels at the center of the gap.

These results are in accordance with experimental results in Meyer and Rehme (1995) and the Reynolds stresses measured in the open water channel by Shiono and Knight (1991), show very similar distribution.

Figure 7 shows the map of isovorticity in the plane of the gap. The vorticity in the XZ plane is given by Eq. (14).

$$\Omega_y = \frac{1}{2} \left[ \left( \frac{\partial u}{\partial z} \right) - \left( \frac{\partial w}{\partial x} \right) \right] \quad (14)$$

Isovorticity values are higher than the expected near the walls. In the extremity of the gap, lines show the presence of a wake like structure, in the region of corresponding to  $z/d=0.8$  to 1.7.

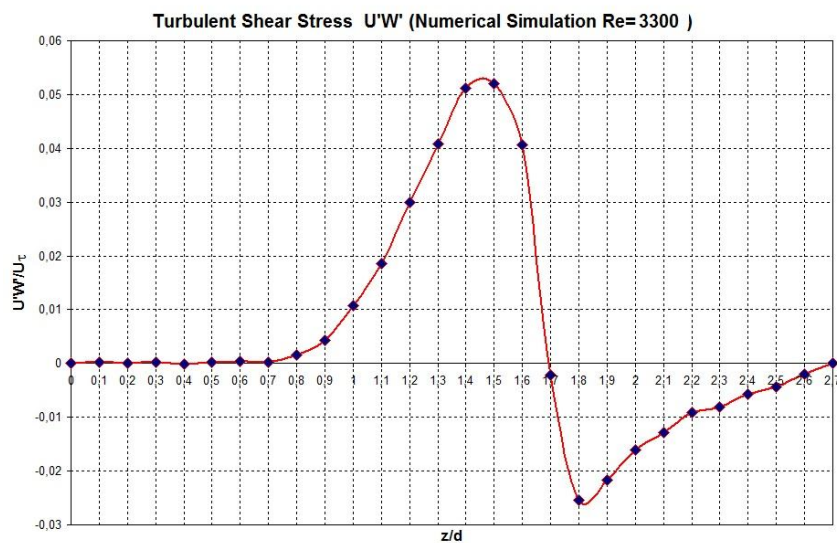


Figure 6. Normalized Turbulent Shear Stress  $U'W'/U\tau$ .

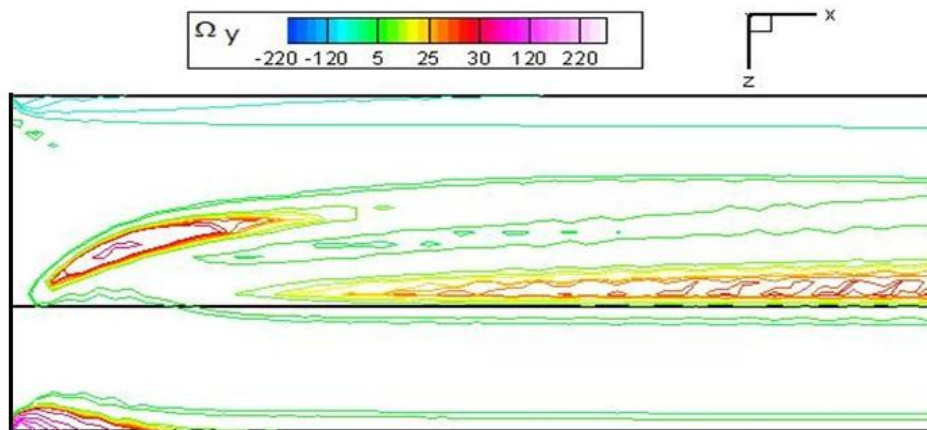


Figure 7. Isovorticity  $\Omega_y$  distribution (numerical:  $Re = 3300$ )

## 5. CONCLUSIONS

This paper presents a finite element computer code for solving the turbulent flow in a compound channel formed by a rectangular cross section region connected to a slot. The numerical methodology is the large eddy simulation with a Smagorinsky model. The turbulent flow is considered quasi-incompressible, isothermal and transient.

The results are consistent with the experimental data. The coarse grid adopted allowed the fast debugging of the code but the velocity in the gap was underestimated. The increase of the Reynolds number will allow direct comparison with the experimental results.

The use of the numerical code applied to the studied problem has shown the ability of this methodology to simulate complex turbulent flows, without limitations on memory allocation, although the very short integration time steps leads to long processing times as the Reynolds number increases. The use of a more refined mesh, now in progress, will bring improvements in flow analysis mainly in the region of the gap.

## 6. ACKNOWLEDGEMENTS

Authors thank the National Center for Supercomputing - Southern Region, Federal University of Rio Grande do Sul (CESUP-RS/UFRGS).

Carla M. Xavier is also grateful to CAPES- Ministry of Education, Brazil, for granting her a fellowship.

## 7. REFERENCES

- Biemüller, M., Meyer, L. and Rehme, K., 1996. "Large eddy simulation and measurement of the structure of turbulence in two rectangular channels connected by the gap", *Engineering Turbulence Modeling and Experiments* 3, Editors: Rodi, W. and Bergeles, G., 249-258.
- Collins, D. C., Williams, M. J., 1959. "Two-dimensional convection from heated wires at low Reynolds numbers. *Journal of Fluid Mechanics*, v. 6, pp. 357-384.
- Findikakis, A.N. and Street, R.L., 1982. "Mathematical Description of Turbulent Flows", *Journal of Hydraulics Division, ASCE*, V108, N°HY8, paper 17265, p887-903.
- Goulart, J. N. V., 2009, "Experimental Study of the Turbulent Shear Flow in Closed Compound Channels" (in Portuguese), Dr. Thesis, PROMEC, Federal University of Rio Grande do Sul, Brazil. Available on line at <http://hdl.handle.net/10183/16204>.
- Hinze, J.O., 1975. "Turbulence", McGraw-Hill, New York.
- Home D., Arvantinis G., Lightstone M. F. and Hamed M. S., 2009, "Simulation of flow pulsations in a twin rectangular subchannel geometry using unsteady Reynolds Averaged Navier-Stokes modeling", *Nuclear Engineering and Design*, 239, pp. 2964-2980.
- Kawahara, M., Hirano, H., 1983. "A Finite Element Method for High Reynolds Number Viscous Fluid Flow Using Two Step Explicit Scheme". *International Journal for Numerical Methods in Fluids*, V.3, pp.137-163.

- Lesieur, M. Comte, P., Métais, O., 1995. "Numerical simulations of coherent vortices in turbulence", ASME - Appl Mech Rev, Vol. 48, N<sup>o</sup>.4.
- Merzari, E., Ninokata, H., Baglietto, E., 2008. "Numerical simulation of flows in tight-lattice fuel bundles". Nucl. Eng. Des. 238, 1703–1719.
- Meyer, L. and Rehme, K., 1995. "Periodic vortices in flow through channels with longitudinal gaps or fins", 10th Symposium on turbulent shear flows, The Pennsylvania State University, University Park, August 14-16.
- Meyer L., 2010. "From discovery to recognition of periodic large scale vortices in rod bundles as source of natural mixing between subchannels - A review", Nuclear Engineering and Design, Vol.240, Issue 6, Pages 1575-1588.
- Möller, S. V., 1991. "On Phenomena of Turbulent Flow through Rod Bundles". Experimental Thermal and Fluid Science, v. 4, n.1, pp. 25-35.
- Olinto, C. R. and Möller, S. 2004. "X-probe calibration using Collis and William's equation". In: 10<sup>o</sup> Congresso Brasileiro de Engenharia e Ciências Térmicas - ENCIT, 2004, Rio de Janeiro.
- Petry A. P., Awruch A. M., 2006, " Large Eddy Simulation of Three-Dimensional Turbulent Flows by the Finite Element Method" . Journal of the Brazilian Society of Mechanical Sciences and Engineering, Vol. XXVIII, pp. 224-232.
- Rowe, D.S., Johnson, B.M. and Knudsen, J. G., 1974. "Implications concerning rod bundle crossflow mixing based on measurements of turbulent flow structure", Int. J. Heat Mass Transfer, 17, 407-419.
- Smagorinsky, J., 1963. "General circulation experiments with the primitive equations. I. The basic experiment", Monthly Weather Reviews, v. 91, pp. 99-164.